Predominance-Zone Diagrams in Solution Chemistry

Dismutation Processes in Two-Component Systems (M–L)

A. Rojas-Hernández, M. T. Ramírez, and I. González

Universidad Autónoma Metropolitana–Iztapalapa, Departmento de Química, Apartado Postal 55-534, 09340 México, D.F. Mexico

J. G. Ibanez

Universidad Iberoamericana, Departmento Ingeniería y Ciencias Químicas, Prolongación Reforma 880,
Lomas de Santa Fe, 01210 México, D. F. Mexico

The concept of disproportionation or dismutation has been frequently used to analyze the stability of intermediate oxidation states of different elements; nevertheless, it has only been used sporadically (usually in a relatively nonsystematic fashion) in processes without electron exchange. A recent paper in *this Journal* explains the construction of predominance-zone diagrams (PZD's) as an important aid for the comprehension of aqueous solution chemistry by using a general donor/acceptor/particle treatment (1). However, the dismutation concept is not dealt with in this reference.

In this paper we show the application of the concept of dismutation in nonredox processes and its relationship to the corresponding chemical-species distribution diagrams and PZD's. During the past few years, we have used this approach in analytical chemistry courses for students majoring in chemical engineering, chemistry, pharmacy, and biochemistry with gratifying results at the Universidad Nacional Autónoma de México as well as at the Universidad Autónoma Metropolitana-Iztapalapa.
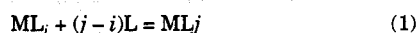
Distribution Diagrams and the Predominance of Chemical Species

Systems of the Type $ML_n/.../ML/M/L$

In aqueous solutions containing two components, M and L, the chemical species,

$$ML, ML_2, ML_3, ..., ML_n$$

can be produced by the following formation equilibria,

$$ML_i + (j - i)L = ML_j \qquad (1)$$

with an associated equilibrium constant,

$$K_{ML_j}^{ML_i,(j-i)L} = \frac{[ML_j]}{[ML_i][L]^{(j-i)}} \qquad (2)$$

$$i \in \{0, 1, 2, ..., (j - 1)\}, \ j \in \{1, 2, ..., n\}$$

This notation includes successive and overall equilibria (2). Other formation equilibria that are useful in some cases are also included.

Taking logs on both sides of this equation and solving for pL (defined as pL = –log [L]), one obtains the following Henderson–Hasselbalch type of equation.

$$pL = \frac{1}{(j-i)}\log\left(K_{ML_j}^{ML_i,(j-i)L}\right) + \frac{1}{(j-i)}\log\left(\frac{[ML_i]}{[ML_j]}\right) \qquad (3)$$

In Charlot's nomenclature (3), ML_n is the polydonor species in the system; M is the polyacceptor; ML, ML_2, ..., $ML_{(n-1)}$ are the ampholytes; and L is the particle. A common, well-known graphical representation for this type of systems is a plot of the molar fractions of the species containing M vs. pL. This is called a chemical-species distribution diagram (4, 5).

Molar Fractions of the Species

The equations of the molar fractions of the species of M depend on the concentration of L as follows.

$$f_M = \frac{[M]}{[M] + [ML] + [ML_2] + ... + [ML_n]}$$

$$= \frac{1}{1 + K_{ML}^{L}[L] + K_{ML_2}^{2L}[L]^2 + ... + K_{ML_n}^{nL}[L]^n} \qquad (4)$$

Table 1. Overall Formation Equilibria and log Values of their Equilibrium Constants for the Systems Used

System	Equilibrium	log β	Ref	System	Equilibrium	log β	Ref
Cu(II)–NH₃	$Cu^{2+} + NH_3 = Cu(NH_3)^{2+}$	4.10	6	Zn(II)–NH₃	$Zn^{2+} + NH_3 = Zn(NH_3)^{2+}$	2.40	6
	$Cu^{2+} + 2NH_3 = Cu(NH_3)_2^{2+}$	7.60			$Zn^{2+} + 2NH_3 = Zn(NH_3)_2^{2+}$	2.30	
	$Cu^{2+} + 3NH_3 = Cu(NH_3)_3^{2+}$	10.50			$Zn^{2+} + 3NH_3 = Zn(NH_3)_3^{2+}$	2.60	
	$Cu^{2+} + 4NH_3 = Cu(NH_3)_4^{2+}$	12.50			$Zn^{2+} + 4NH_3 = Zn(NH_3)_4^{2+}$	2.10	
Proton–phosphates	$PO_4^{3-} + H^+ = HPO_4^{2-}$	12.34	6	Mn(II)–oxalates	$Mn^{2+} + Ox^{2-} = MnOx$	2.40	7
	$PO_4^{3-} + 2H^+ = H_2PO_4^{-}$	19.54			$Mn^{2+} + 2Ox^{2-} = Mn(Ox)_2^{2-}$	5.66	
	$PO_4^{3-} + 3H^+ = H_3PO_4$	21.68			$Mn^{2+} + 3Ox^{2-} = Mn(Ox)_3^{4-}$	6.00	
Ag(I)–NH₃	$Ag^+ + NH_3 = Ag(NH_3)^+$	3.30	6	Fe(II)–(o-phen)	$Fe^{2+} + o\text{-phen} = Fe(o\text{-phen})^{2+}$	5.84	7
	$Ag^+ + 2NH_3 = Ag(NH_3)_2^+$	7.20			$Fe^{2+} + 2o\text{-phen} = Fe(o\text{-phen})_2^{2+}$	11.20	
					$Fe^{2+} + 3o\text{-phen} = Fe(o\text{-phen})_3^{2+}$	21.30	
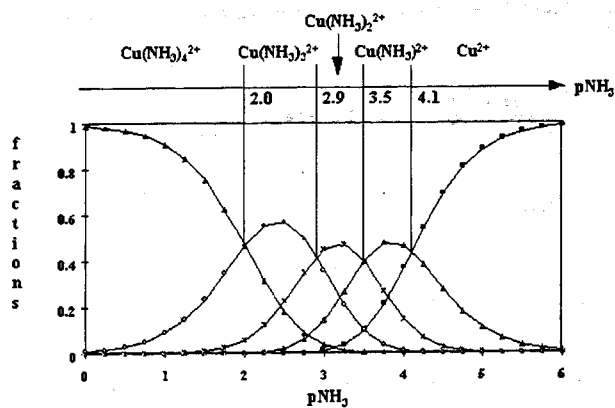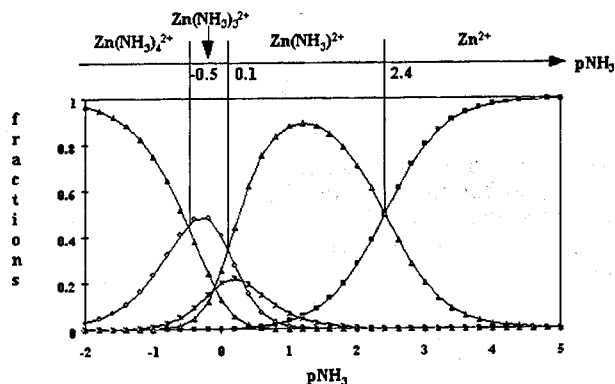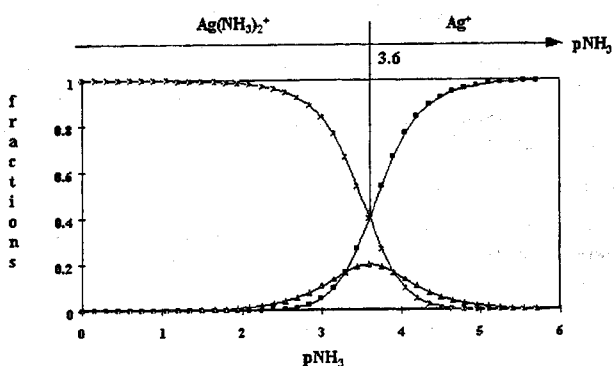
Figure 1. Chemical-species distribution diagrams for some metal cation systems as a function of pNH_3. (a) Cu(II)–NH_3. (b) Zn(II)–NH_3. (c) Ag(I)–NH_3. (■ fraction of M, △ fraction of ML, × fraction of ML_2, ○ fraction of ML_3, and ▲ fraction of ML_4. The PZD's above each distribution diagram are obtained by projecting the intersection points of the greatest fractions over the pNH_3 scale.)

and

$$f_{ML_j} \equiv \frac{[ML_j]}{[M] + [ML] + \ldots + [ML_n]} = f_M K^L_{ML_j}[L]^j \qquad (5)$$

$$i \in \{1, 2, \ldots, n\}$$

These functions are monotonic with respect to [L] (or to pL) for the polyacceptor as well as for the polydonor because the functions in their denominators are polynomials containing only integer exponentials (positive for M, negative for ML_n). However, the functions for the ampholytes present a maximum because here each polynomial presents integer exponents that are both positive and negative when the expression is simplified with the numerator.
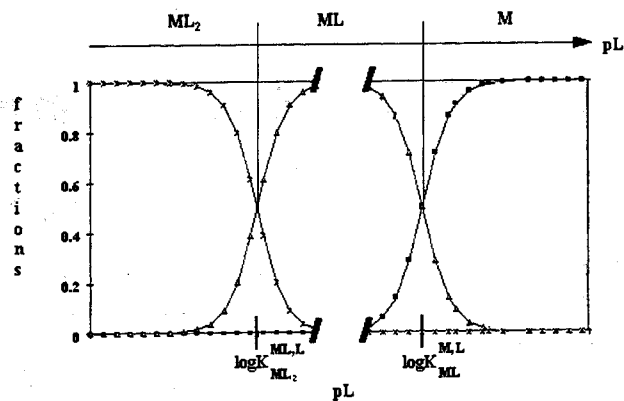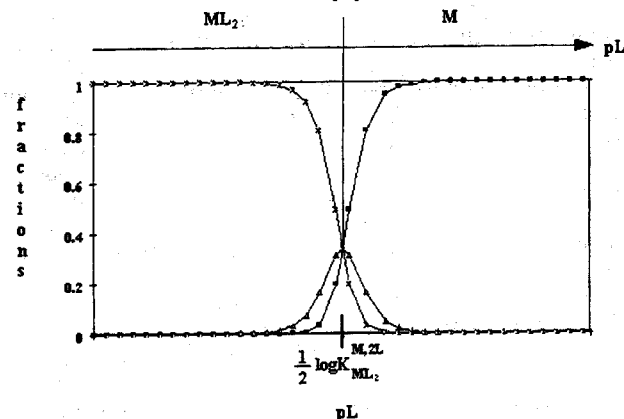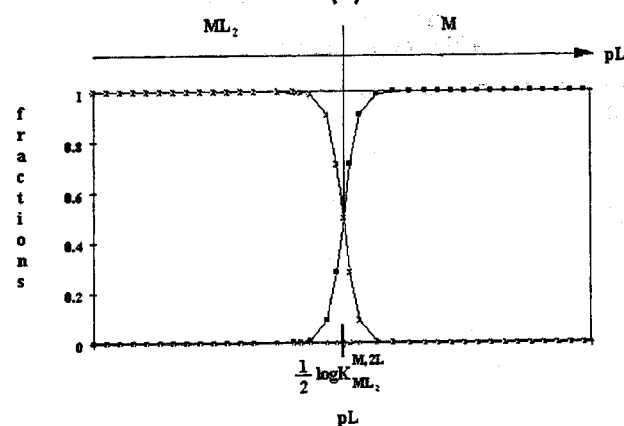
Figure 2. Distribution diagrams and PZD's for systems of the type $ML_2/ML/M/L$. (a) Limiting case, where $\log K^{ML,L}_{ML_2} \ll \log K^{M,L}_{ML}$ or $\log K^{2ML}_{ML_2,M} \ll 0$. (b) Case where $\log K^{ML,L}_{ML_2} = \log K^{M,L}_{ML}$ or $\log K^{2ML}_{ML_2,M} = 0$. (c) Limiting case where $\log K^{ML,L}_{ML_2} \gg \log K^{M,L}_{ML}$ or $\log K^{2ML}_{ML_2,M} \gg 0$. (■ fraction of M, △ fraction of ML, and × fraction of ML_2.)

When the fraction of ML_j is larger than that of all the other species that contain M, then ML_j is said to predominate in the system. The chemical-species distribution diagrams shown throughout this paper can be easily constructed by introducing eqs 4 and 5 in a spreadsheet (e.g., Excel 4.0, Microsoft) and using equilibrium constants reported in the literature (6, 7). Table 1 shows the values of the equilibrium constants of the systems discussed in this paper.

Table 2. Dismutation Equilibria of the Ampholytes in the Systems

Proton–Phosphates, Manganese(II)–Oxalates (Ox)
and Iron(II)–*ortho*-Phenanthroline (*o*-phen)
with Corresponding Values of the log of the Equilibrium Constants

Ampholyte	Dismutation Equilibrium	log K
HPO_4^{2-}	$2HPO_4^{2-} = H_2PO_4^- + PO_4^{3-}$	−5.1
	$3HPO_4^{2-} = H_3PO_4 + 2PO_4^{3-}$	−15.3
$H_2PO_4^-$	$2H_2PO_4^- = H_3PO_4 + HPO_4^{2-}$	−5.1
	$3H_2PO_4^- = 2H_3PO_4 + PO_4^{3-}$	−15.3
MnOx	$2MnOx = MnOx_2^{2-} + Mn^{2+}$	0.8
	$3MnOx = MnOx_3^{4-} + 2Mn^{2+}$	−1.2
$MnOx_2^{2-}$	$2MnOx_2^{2-} = MnOx_3^{4-} + MnOx$	−2.9
	$3MnOx_2^{2-} = 2MnOx_3^{4-} + Mn^{2+}$	−5.0
$Fe(o\text{-phen})^{2+}$	$2Fe(o\text{-phen})^{2+} = Fe(o\text{-phen})_2^{2+} + Fe^{2+}$	−0.5
	$Fe(o\text{-phen})^{2+} = Fe(o\text{-phen})_3^{2+} + 2Fe^{2+}$	3.78
	$2Fe(o\text{-phen})_2^{2+} = Fe(o\text{-phen})_3^{2+}$ $+ Fe(o\text{-phen})^2$	4.7
$Fe(o\text{-phen})_2^{2+}$	$3Fe(o\text{-phen})_2^{2+} = Fe(o\text{-phen})_3^{2+} + Fe^{2+}$	9.0

In Figure 1 some distribution diagrams of metallic cations (Cu(II), Zn(II), and Ag(I)) with ammonia are shown. In the case of copper, all of the species can predominate in a given pNH3 interval. On the contrary, in the cases of silver and zinc the species monoamminesilver and diamminezinc cannot predominate anywhere even though they are present in the system; thus it cannot be said that they do not exist.

Although this type of system (where not all the existing species have a predominance zone in the pL scale) is not considered in the paper mentioned above (*1*), PZD's can be constructed for them. Suffice it to observe the pL interval for which the fraction of one species is larger than any other in order to construct the PZD of M-containing species in the system.

The Points of Intersection

The points of intersection of the fractions of the species ML_i and ML_j are given by the values of

$$pL = \frac{1}{(j-i)}\log K_{ML_j}^{ML_i,(j-i)L}$$

according to the Henderson–Hasselbalch type of equation.

The upper part of Figure 1 also shows how the PZD's of the Cu(II), Ag(I), and Zn(II) systems can be obtained as projections of the intersection points of the largest fractions on the pNH3 scale. At these points, the molar fractions of the predominant species become equal. Vale et al. (*1*) call these points acceptance potentials; they mark the predominance boundaries of the chemical species. Although PZD's can be constructed this way, this method does not show why some ampholytes cannot predominate in the system.

Dismutation Equilibria and Ampholyte Stability

Ampholytes can react both as particle donors and acceptors; this enables them to react with themselves under some circumstances. Charlot (*3*) has pointed out that it is useful to include the dismutation of ampholytes to simplify
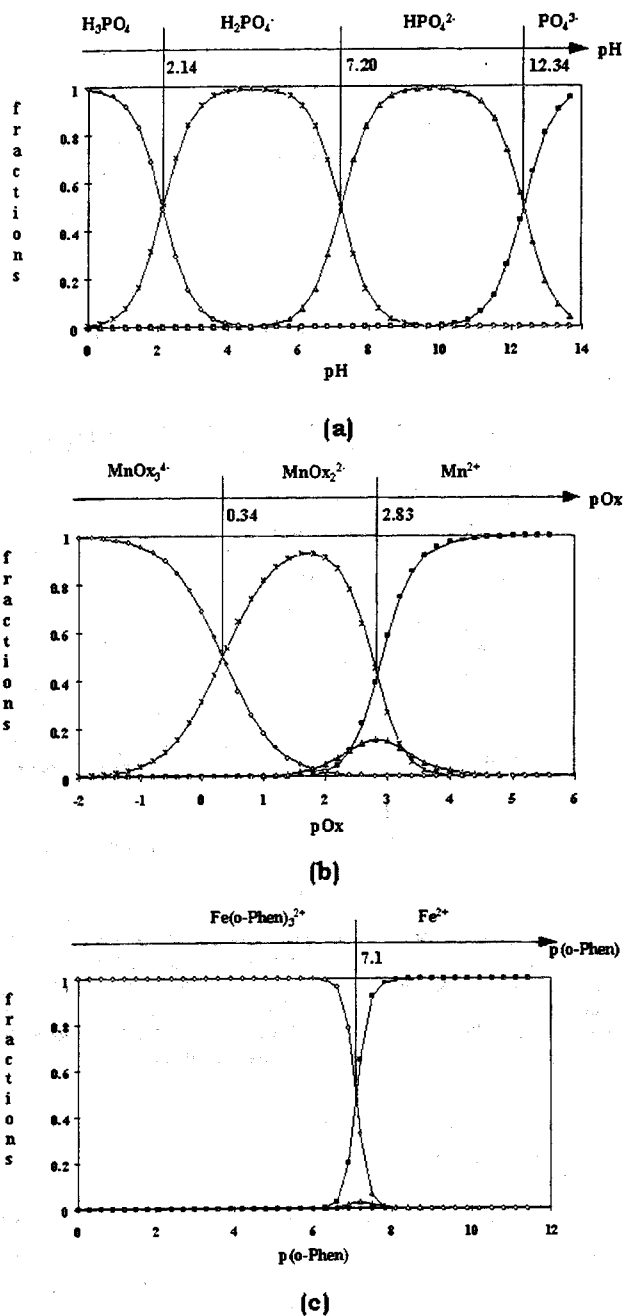

Figure 3. Sample distribution and PZD's for systems of the type $ML_3/ML_2/ML/M/L$. (a) proton–phosphates, (b) Mn(II)–Ox, (c) Fe(II)–(*o*-phen). (■ fraction of M, △ fraction of ML, × fraction of ML_2, and ○ fraction of ML_3.)

the analysis of polydonor/ampholyte(s)/polyacceptor/particle systems. This is shown below.

Two-Particle Donors (ML2/ML/M/L)

Here, there is only one ampholyte (ML) with one dismutation equilibrium.

$$2ML = ML_2 + M \tag{6}$$

and with an associated equilibrium constant given by

$$K_{ML_2,M}^{2ML} = \frac{[ML_2][M]}{[ML]^2} \tag{7}$$

Two possibilities arise from this: Either the ampholyte can predominate in the system (Fig. 2a), or it cannot predominate (Figs. 2b and 2c). This information can be obtained from the value of the dismutation constant of the
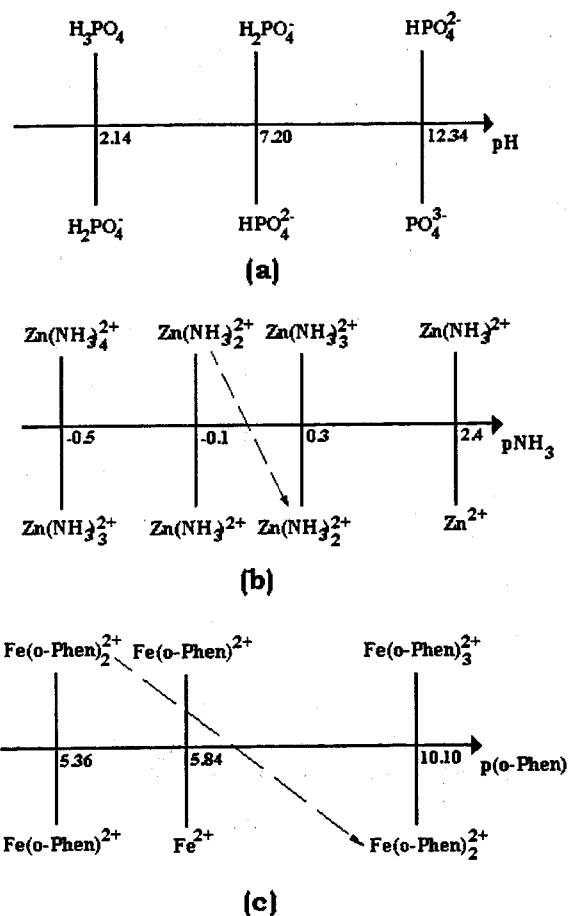
(a)

(b)

(c)

Figure 4. Placement of the successive donor/acceptor pairs of different systems according to the points a, b, and c of Charlot's convention (3). (a) proton-phosphates system on the pH scale, (b) $Zn(II)$–NH_3 system on the pNH_3 scale, (c) $Fe(II)$–(o-phen) system on the $p(o$-phen) scale. The dotted diagonal arrows signal ampholyte dismutation processes with equilibrium constants greater than 1.

ampholyte, as shown in Figure 2. Then, in this type of system ML can predominate in some interval of pL values if and only if

$$\log K^{2ML}_{ML_2,M} < 0 \qquad (8)$$

For example, the system Ag(I)–NH_3 has an ampholyte with a dismutation equilibrium,
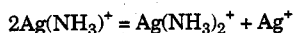
$$2Ag(NH_3)^+ = Ag(NH_3)_2{}^+ + Ag^+$$

and an equilibrium constant,

$$K^{2Ag(NH_3)^+}_{Ag(NH_3)_2,Ag^+} = \frac{[Ag(NH_3)_2^+][Ag^+]}{[Ag(NH_3)^+]^2} = 10^{0.6} > 1$$

obtained from Hess' law by using known equilibrium constants shown in Table 1. Because this dismutation constant is greater than unity, the ampholyte cannot predominate (Fig. 1c).

Three-Particle Donor Systems (ML_3/ML_2/ML/M/L)

Here, there are two ampholytes (ML_2 and ML). Each one participates in two different dismutation equilibria. Table 2 shows the possible dismutation equilibria for the ampholytes in three selected example systems: phosphoric acid, Mn(II)–oxalate and Fe(II)–o-phenanthroline . The corresponding distribution diagrams are shown in Figure 3.

The information in Table 2 and the shape of the distribution diagrams in Figure 3 show that if at least one of the dismutation constants of a given ampholyte is greater that
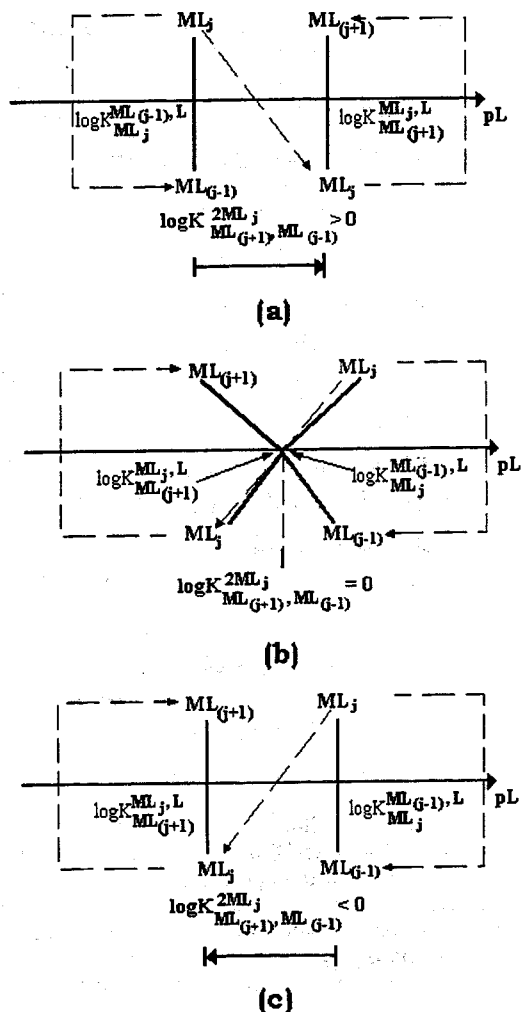

(a)

(b)

(c)

Figure 5. Graphical representation of dismutation equilibria of the type $2ML_j = ML_{(j+1)} + ML_{(j-1)}$ according to Charlot's convention for the prediction of reactions (3). (a) The ampholyte ML_j dismutates with $\log K^{2ML_j}_{ML_{(j+1)},ML_{(j-1)}} > 0$ and thus cannot predominate in the system. (b) The ampholyte ML_j dismutates with $\log K^{2ML_j}_{ML_{(j+1)},ML_{(j-1)}} = 0$ and thus cannot predominate in the system. (The lines joining the donor/acceptor pairs must bend because both pairs are located at the same point.) (c) The ampholyte ML_j dismutates with $\log K^{2ML_j}_{ML_{(j+1)},ML_{(j-1)}} < 0$ and can predominate in the interval $\log K^{ML_j,L}_{ML_{(j+1)}} < pL < \log K^{ML_{(j-1)},L}_{ML_j}$. The donor points toward the acceptor, and they produce their corresponding conjugated products. The short and thick arrows define the direction of the vector, which is defined by the sign of $\log K^{2ML_j}_{ML_{(j+1)},ML_{(j-1)}}$.

unity (i.e., $\log K > 0$), then that ampholyte cannot predominate in the system.

Multiparticle Donor Systems (ML_n/.../ML/M/L)

In general, for multiparticle donor systems there are $(n - 1)$ ampholytes with dismutation equilibria of the type,

$$(k - i)ML_j = (j - i)ML_k + (k - j)ML_i \qquad (9)$$

and their equilibrium constants are written as

$$K^{(k-i)ML_j}_{(j-i)ML_k,(k-j)ML_i} = \frac{[ML_k]^{(j-i)}[ML_i]^{(k-j)}}{[ML_j]^{(k-i)}} \qquad (10)$$

$$i \in \{0, 1, 2, ..., (j-1)\}$$
$$j \in \{1, 2, ..., (n-1)\}$$
$$k \in \{(j+1), (j+2), ..., n\}$$

It is relatively easy to demonstrate that in this general case, the ampholyte ML_j can have up to $j(n-j)$ different dismutation processes; this can be shown by counting the number of species before and after this ampholyte, according to the following sequence.

$$\underbrace{M, ML, ..., ML_{(j-1)}, ML_j,}_{j \text{ species}} \underbrace{ML_{(j+1)}, ..., ML_n}_{(n-j) \text{ species}}$$
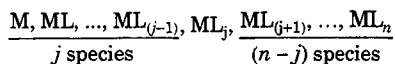
In this way, the total number of different dismutation processes (NDP's) is equal to the sum of the individual possible dismutation processes of each ampholyte.

$$NDP = \sum_{j=1}^{n-1} j(n-j) = n\sum_{j=1}^{n-1} j - \sum_{j=1}^{n-1} j^2 = \frac{n(n^2-1)}{6} \quad (11)$$

Only $(n-1)$ dismutation equilibria can be used to gather a set of n independent equilibria (8) to thermodynamically describe these systems.

In addition, as a general rule, an ampholyte cannot predominate in a system where at least one of its dismutation constants is greater than or equal to 1. For this reason, dismutation equilibria can be considered as stability criteria of ampholytes.

Charlot's Scale for the Prediction of Reactions

The calculation of the constants of all the dismutation equilibria present in a given system to determine which ampholytes cannot predominate could become cumbersome; the total number of equilibria could be very large. For example, for a hexadonor system of the type

$$ML_6/.../ML/M/L \qquad n = 6$$

there are 35 different dismutation equilibria, according to the calculation described above (eq 11). For this reason, Charlot (3) and Trémillon (9) devised a graphic algorithm that facilitates the successive and exhaustive selection of only the dismutation equilibria of ampholytes that cannot predominate in the system. We now describe the convention for Charlot's scale for the prediction of reactions and its application to the construction of PZD's.

Charlot's Convention for the Scale for Predicting Reactions as Applied to Construction of PZD's
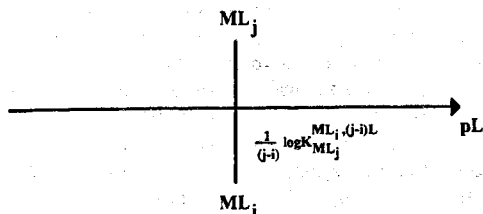
a. Scale

The scale for the prediction of reactions is a linear pL scale.

b. Positioning a Donor/Acceptor Pair on the Scale

The conjugated donor/acceptor pairs like those of eq 1 are placed on the pL scale at the point where $[ML_i] = [ML_j]$ because this implies that

$$pL = \frac{1}{(j-i)} \log K_{ML_j}^{ML_i,(j-i)L}$$

according to the Henderson–Hasselbalch type equation (eq 3). Donors are placed on the upper part, and the acceptors are on the lower part. Then, the placement of this pair on the scale looks like

Here, ML_j is the conjugated donor of ML_i (1, 10, 11). In order for this scale to have a practical application, it is nec-

essary to establish the type of pairs that must be placed on it.

c. Use of the Scale for a Polydonor System of the Type $ML_n/.../ML/M/L$

c.1 Placement of the Successive Donor/Acceptor Conjugated Pairs.

Each pair of the set of independent successive equilibria ($ML_{(j-1)} + L = ML_j$) is placed on the scale. The Henderson–Hasselbalch type equation used for each donor/conjugated acceptor pair is

$$pL = \log K_{ML_j}^{ML_{(j-1)},L} + \log \left(\frac{[ML_{(j-1)}]}{[ML_j]} \right)$$

Then, when $[ML_{(j-1)}] = [ML_j]$,

$$pL = \log K_{ML_j}^{ML_{(j-1)},L}$$

For Brönsted acids and bases, pK_a values (that correspond to successive dissociation equilibria) are usually reported; whereas, $\log \beta$ values (that correspond to global formation equilibria constants) are reported for coordination compounds. For this reason, care must be taken when using these data. Hess' law can be used when necessary to obtain successive constants from global constants and vice versa.
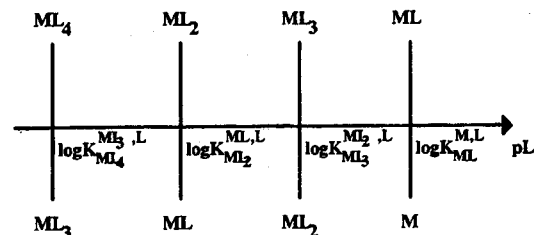
Figure 4 shows some examples of the placement of successive formation equilibria in different systems. As shown, the successive formation equilibria of the proton–phosphate system follow the statistically expected order (12), that is,

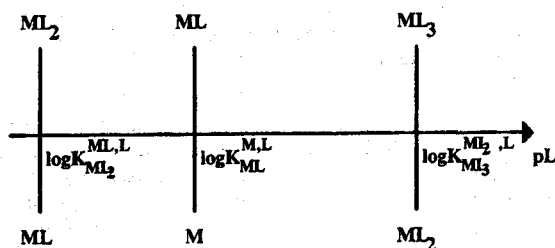$$\log K_{ML_3}^{ML_2,L} < \log K_{ML_2}^{ML,L} < \log K_{ML}^{M,L}$$
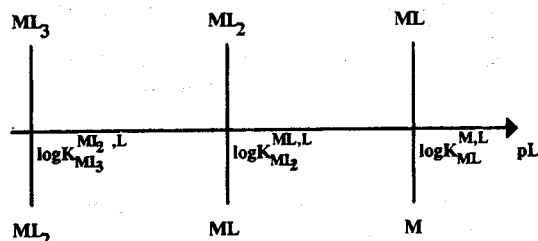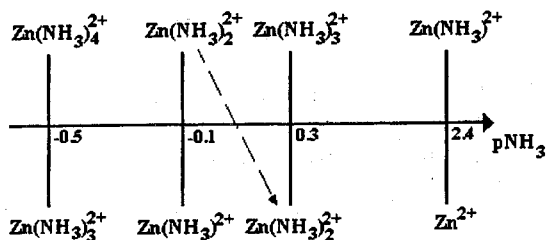

In the system Zn(II)–NH₃,

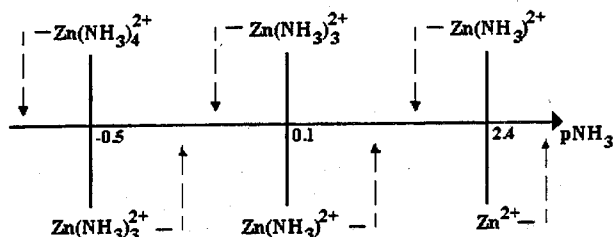$$\log K_{ML_4}^{ML_3,L} < \log K_{ML_2}^{ML,L} < \log K_{ML_3}^{ML_2,L} < \log K_{ML}^{M,L}$$

In the system Fe(II)–(o-phen),

$$\log K_{ML_2}^{ML,L} < \log K_{ML}^{M,L} < \log K_{ML_3}^{ML_2,L}$$

(a)

(b)

Figure 6. Simplification of the scale for the prediction of reactions of the system $Zn(II)–NH_3$ according to the points d and e of Charlot's convention (3). (a) Initial scale. (b) First and last scale simplification. (Dotted arrows show the assignment of species to their respective predominance zones.)

These graphical representations, developed from the convention points described above, show some chemical reactions and the log values of their equilibrium constants as well as some dismutation equilibria that are described below.

c.2 Directed Distance. It is well-known that the log value of the equilibrium constant of the following dismutation equilibria,
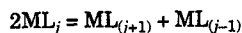
$$2ML_j = ML_{(j+1)} + ML_{(j-1)}$$

can be obtained by using Hess' law and combining the corresponding successive equilibria as follows.

$$ML_j = ML_{(j-1)} + L \qquad \log K = -\log K_{ML_j}^{ML_{(j-1)},\,L}$$

$$\underline{ML_j + L = ML_{(j+1)} \qquad \log K = +\log K_{ML_{(j+1)}}^{ML_j,\,L}}$$

$$2ML_j = ML_{(j+1)} + ML_{(j-1)} \qquad \log K_{ML_{(j+1)},\,ML_{(j-1)}}^{2ML_j} = +\log K_{ML_{(j+1)}}^{ML_j,\,L} - \log K_{ML_j}^{ML_{(j-1)},\,L}$$

The sign of the term,

$$\log K_{ML_{(j+1)},ML_{(j-1)}}^{2ML_j}$$

depends upon the values of

$$\log K_{ML_{(j+1)}}^{ML_j,L}$$
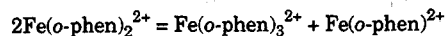
and

$$\log K_{ML_j}^{ML_{(j-1)},L}$$

Because successive equilibria have been graphically represented at $pL = \log K$, with the donors on the upper side and with the acceptors on the lower side, the values of $\log K_{ML_{(j+1)},ML_{(j-1)}}^{2ML_j}$ and their signs have also been represented, as shown in Figure 5. Here, it is also shown that this convention defines directed distances among the pairs; it defines vectors. So this scale is just a graphical representation of Hess' law like any other graphical method of prediction of reactions ($13, 14$). Then, Figure 4b shows that the equilibrium constant for the dismutation,

$$2Zn(NH_3)_2{}^{2+} = Zn(NH_3)_3{}^{2+} + Zn(NH_3){}^{2+}$$
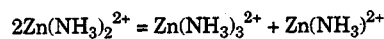
is greater that 1 and so is that of the dismutation,

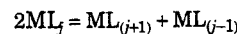$$2Fe(o\text{-phen})_2{}^{2+} = Fe(o\text{-phen})_3{}^{2+} + Fe(o\text{-phen}){}^{2+}$$

according to Figure 4c.

d. PZD's from the Scale of Prediction of Reactions

From here, two possibilities arise.

d.1 All the dismutation constants corresponding to the equilibria of the type

$$2ML_j = ML_{(j+1)} + ML_{(j-1)}$$

(named here as stoichiometry 2:1:1) are less than 1. Thus, all the ampholytes can predominate according to the statistically expected order shown below.

Then, the PZD is as follows.
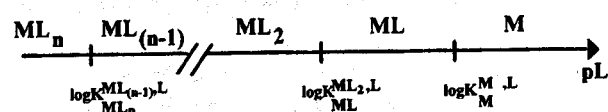
d.2 One or more dismutation constants of 2:1:1 stoichiometry, represented on the scale, are greater than 1.

In these cases, a simplification procedure must be used to obtain the corresponding PZD, as explained below.

e. Simplification of the Scale for the Prediction of Reactions

e.1 Identification. Among the ampholytes with equilibrium constants greater than 1, the most unstable—that is, the one with the largest dismutation constant (e.g., ML_j)—is selected.

e.2 Substitution. Those pairs containing the most unstable ampholyte, ML_j are removed from the scale and substituted with the pair that involves the products (ML_i and ML_k) from the dismutation equilibrium that prevents ML_j from predominating in the system ($3, 9$).

e.3 Exhaustive Repetition. Points *e.1* and *e.2* are then repeated until there are no more ampholytes in the scale with dismutation equilibrium constants greater than or equal to 1 or until there are no more ampholytes there.

e.4 PZD's. The PZD is then constructed from the simplified scale, following the statistically expected order for the predominance of species. An example of a PZD thus obtained is
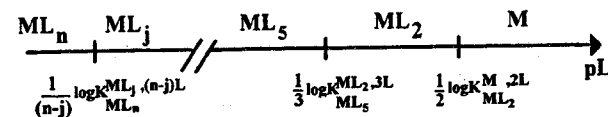

Figure 4a shows that it is not necessary to simplify the scale of the system proton–phosphates. Figures 4b and 4c show that it is necessary to use the procedure described above for the systems $Zn(II)–NH_3$ and $Fe(II)–(o\text{-phen})$. Examples of the simplification procedure described above (i.e., point e of the convention) and the corresponding PZD's are given in Figures 6 and 7. The simplification process in Figure 6 is stopped when the ampholyte $Zn(NH_3)_2{}^{2+}$ is removed from the scale for the prediction of reactions because all the constants of the dismutation equilibria of the other two ampholytes ($Zn(NH_3){}^{2+}$ and $Zn(NH_3)_3{}^{2+}$) are less than 1.On the contrary, the scale for the system
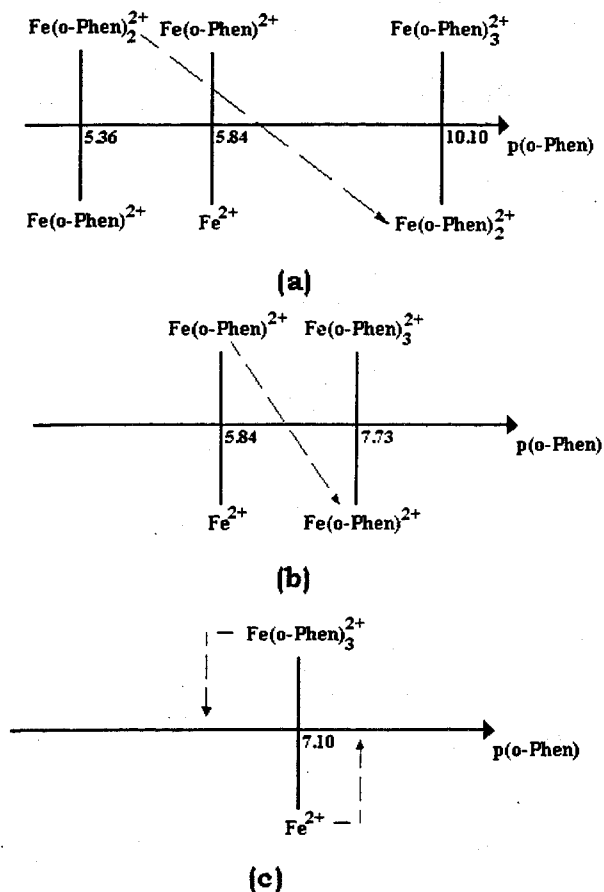
Figure 7. Simplification of the scale for the prediction of reactions of the system Fe(II)–(o-phen) according to the points d and e of Charlot's convention (3). (a) Initial scale. (b) First scale simplification showing the dismutation of the ampholyte Fe(o-phen)$^{2+}$. (c) Second and last scale simplification. (Dotted arrows signal the assignment of species to their corresponding predominance zones.)

Fe(II)–(o-phen) must be simplified twice, as shown in Figure 7. This can be understood in the light of the above discussion by looking at the corresponding data in Table 2.

In Figure 7b the dismutation equilibrium constant for

$$\tfrac{3}{2}Fe(o\text{-phen})^{2+} = \tfrac{1}{2}Fe(o\text{-phen})_3^{2+} + Fe^{2+}$$
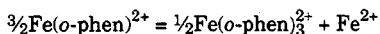
(not plotted in Figures 7a nor 7c) is greater than 1,

$$\log K^{\tfrac{3}{2}Fe(o\text{-phen})_2^{2+}}_{\tfrac{1}{2}Fe(o\text{-phen})_3^{2+},Fe^{2+}} = 1.89 > 0$$

Then, the constant for the equilibrium $3Fe(o\text{-phen})^{2+} = Fe(o\text{-phen})_3^{2+} + 2Fe^{2+}$ (which represents the same dismutation process) is also greater than 1,

$$\log K^{3Fe(o\text{-phen})_2^{2+}}_{Fe(o\text{-phen})_3^{2+},2Fe^{2+}} = 3.78 > 0$$

In the simplified scales for the prediction of reactions that appear along the procedure outlined in point e of the convention, some of the dismutation processes thereby represented no longer have a 2:1:1 stoichiometry. Care must be used with the interpretation of the dismutation processes represented in the simplified scales.

Observations

Charlot's convention for the scale for the prediction of reactions is more comprehensive and powerful than we have shown in this limited space because the pL scale contains more than the dismutation equilibria, that is, other reaction equilibria among donors and nonconjugated acceptors not discussed here. The directed distance (defined in points a and

b of the convention) is applicable to other equilibria in addition to the dismutation cases discussed here.

Other points of the convention (not treated here) allow for the placement of the particle L on the pL scale as well as for the overlap of all the necessary reduced scales in order to describe the composition of the solution. This enables the prediction of reactions in polydonor systems that exchange the same particle L, for example,

$$ML_n/.../ML/M/L, \quad AL_a/.../AL/A/L, \quad BL_b/.../BL/B/L$$
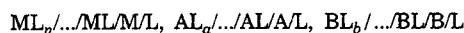
This leads to adequate models for the calculation of equilibrium compositions in systems involved in processes such as titrations, hydrometallurgy, biochemistry, and processes in aqueous solutions in general (3, 9).

The complete Charlot's convention is not presented here due to space limitations and because our main objective is to emphasize the importance of the dismutation processes in the construction of PZD's. We have used Ringbom's nomenclature (15) for the labeling of the different equilibrium constants in an attempt to use one single convention because the IUPAC has not established a convention for writing equilibrium constants of dismutation processes.

Conclusions

The main contribution of the concept of dismutation equilibria as applied to solution chemistry is that it explains the nonpredominance of some ampholytes in a given system. The use of these equilibria combined with another graphical method of prediction of reactions (3, 9, 13, 14), can lead to the construction of PZD's without having to use the corresponding chemical-species distribution diagrams.

The PZD's discussed here (and earlier (1)), describe two-component systems. Actually, real-life chemical processes usually involve more than two components; nonetheless, the algorithm discussed here can be generalized for multi-component, multireacting systems in aqueous solutions by considering the formation of mixed complexes (16, 17), polynuclear species (18), condensed-phase equilibria (19, 20) and electron exchange (redox systems) (21).

Literature Cited

1. Vale, J.; Fernández-Pereira, C.; Alcalde, M. *J. Chem. Educ.* **1993**, *70*, 790–795.
2. Lagowski, J. J. *Modern Inorganic Chemistry*; Dekker: New York, 1973; Chapter 17.
3. Charlot, G. *Chimie Analytique Générale*, Part I; Masson: Paris, 1967.
4. Kolthoff, I. M.; Sandell, E. B.; Meehan, E. J.; Bruckenstein, S. *Quantitative Chemical Analysis*; MacMillan: London, 1969.
5. Högfeldt, E. In *Treatise on Analytical Chemistry*; Kolthoff, I. M.; Elving, P. J., Eds; Interscience: New York, 1979; Part 1, Vol. 2, Section D (Continued), Chapter 15.
6. Högfeldt, E. *Stability Constants of Metal–Ion Complexes*: Part A: Inorganic Ligands (IUPAC Chemical Data Series, No. 21); Pergamon: New York, 1979.
7. Perrin, D. D. *Stability Constants of Metal–Ion Complexes*: Part B: Organic Ligands (IUPAC Chemical Data Series, No. 22); Pergamon: New York, 1979.
8. Smith, W. R.; Missen, R. W. *Chemical Reaction Equilibrium Analysis: Theory and Algorithms*; Wiley: New York, 1985.
9. Trémillon, B. *Électrochimie Analytique et Réactions en Solution. Volume 1: Réactions en Solution*; Masson: Paris, 1993.
10. Pacer, R. A. *J. Chem. Educ.* **1973**, *50*, 178–180.
11. Elenkova, N. G. *Talanta* **1980**, *27*, 699–704.
12. Holzbecher, Z.; Diviš, L.; Král, M.; Šucha, L.; Vláčil, F. *Handbook of Organic Reagents in Inorganic Analysis*; Kotrlý Translator; Horwood: New York, 1976, Chapter 3.
13. Latimer, W. M.; *Oxidation Potentials*, 2nd ed.; Prentice-Hall: Englewood Cliffs, NJ, 1952.
14. Frost, A. A. *J. Am. Chem. Soc.* **1951**, *73*, 2680–2683.
15. Ringbom, A. *Complexation in Analytical Chemistry*; Wiley: New York, 1963.
16. Rojas, A.; González, I. *Anal. Chim. Acta* **1986**, *187*, 279–285.
17. Rojas-Hernández, A.; Ramírez, M. T.; Ibanez, J. G.; González, I. *Anal. Chim. Acta* **1991**, *246*, 435–442.
18. Rojas-Hernández, A.; Ramírez, M. T.; González, I.; Ibanez, J. G. *Anal. Chim. Acta* **1992**, *259*, 95–104.
19. Rojas-Hernández, A.; Ramírez, M. T.; González, I. *Anal. Chim. Acta* **1993**, *278*, 321–333.
20. Rojas-Hernández, A.; Ramírez, M. T.; González, I. *Anal. Chim. Acta* **1993**, *278*, 335–347.
21. Rojas-Hernández, A.; Ramírez, M. T.; Ibanez, J. G.; González, I. *J. Electrochem. Soc.* **1991**, *138*, 365–371.